THE PENNSYLVANIA STATE UNIVERSITY
SCHREYER HONORS COLLEGE

DEPARTMENT OF CHEMICAL ENGINEERING

Electrocatalytic properties of an iron organometallic complex and its role in the reduction of nitroaromatic compounds

JOSHUA MILLER
SPRING 2022

A thesis
submitted in partial fulfillment
of the requirements
for a baccalaureate degree
in Chemical Engineering
with honors in Chemical Engineering

Reviewed and approved* by the following:

Michael John Janik
Professor of Chemical Engineering
Thesis Supervisor

Ali Borhan
Professor of Chemical Engineering
Honors Adviser

* Electronic approvals are on file.

ABSTRACT

The electrochemical properties and electrocatalytic activity of an iron organometallic complex were investigated using Density Functional Theory (DFT) methods. The complex was studied for the electrocatalytic reduction of nitroaromatic compounds. The complex contains a central iron atom bound to two chelated ligands, each containing two nitrogen atoms and one oxygen atom connected to iron. In the most oxidized state of the complex, the iron lacks an open coordination site for substrate binding. Upon addition of an electron and proton to a nitrogen on one of the ligands, an iron-oxygen bond dissociates, leading to the ligand shifting away from the iron. Five atoms remain bound to the iron, meaning there is an open coordination site. This freeing of a coordination site allows an inner-sphere mechanism to take place for the electrocatalytic reduction of nitroaromatics, namely nitrobenzene and TNT. Complexation of nitrobenzene with the catalyst provided energetic stabilization. The inner-sphere catalytic mechanism for nitrobenzene reduction mostly proceeded downhill energetically, with the initial reduction of the catalyst to free a coordination site being the rate-limiting step. TNT electrocatalytic reduction by the iron organometallic complex followed a similar pattern, with the removal of OH from the catalyst being the rate-limiting step.

TABLE OF CONTENTS

LIST OF FIGURES

LIST OF TABLES

ACKNOWLEDGEMENTS

I would like to thank Dr. Michael Janik for his tremendous support and guidance during my time in his lab. Working in Dr. Janik's lab has given me the opportunity to grow academically and professionally, helping me develop a passion for research and creative problem-solving. I could not ask for a more caring and dedicated adviser. I would also like to thank Andrew Wong for training me in various computational methods and guiding me through this project. I am very grateful to have such a supportive mentor who helped me expand my research skills and abilities. I would like to thank Brandon Perdue for working with me in the Janik lab over the past three years, providing encouragement and overcoming challenges together. I also would like to thank the entire Janik lab for all their assistance with my research and for being such a welcoming team.

I would like to thank The Penn State University Department of Chemical Engineering for helping grow my intellectual curiosity related to the field of chemical engineering. I would like to thank the Schreyer Honors College for affording me the opportunity to pursue this valuable research experience and an undergraduate honors thesis. I would also like to thank the Institute for Computational and Data Sciences at Penn State for providing computational resources that made this project possible.

Finally, I would like to thank my family and friends for their tireless support and encouragement during my four years at Penn State.

Chapter 1

Introduction

Nitroaromatics in wastewater pose risks to both the environment and human health, and these risks can be mitigated by converting nitroaromatics to more benign products. Nitroaromatic compounds such as 2,4,6-trinitrotoluene (TNT) and nitrobenzene contribute to the contamination of soil and groundwater. They are also toxic to many aquatic species.[1] From a human health perspective, TNT is a mutagenic compound, capable of inducing hemolysis and hepatotoxicity in humans.[1] One common route of detoxifying nitroaromatics entails reducing their nitro groups to amines. Aromatic amines are generally more benign and biodegradable than nitroaromatics.[1] Additionally, aromatic amines are used in many industrial settings. For instance, aniline, the reduction product of nitrobenzene, is a valuable chemical used to produce pharmaceuticals, dyes, pigments, and pesticides.[2] It also has some toxicity but can be easily detoxified via oxidation to insoluble oligomers.[1]

There are various methods for reducing nitroaromatics, but electrochemical treatment holds many advantages over other alternatives. Biological treatment of nitroaromatics is limited because hazardous byproducts can form and nitroaromatics are toxic to microorganisms.[1] Meanwhile, chemical treatment is energy-intensive and may release NO_x emissions, which are of environmental concern.[1] In contrast to biological and chemical treatment, electrocatalysis is a favorable choice for many reasons[1]: it is cost-effective and environmentally sustainable, with electrical energy supplied to drive the reaction. Additionally, an electrocatalytic reaction can be

run at convenient operating conditions (low temperature, pressure), and can be engineered to increase selectivity towards a desired product.

In this study, an iron organometallic complex, with an iron center and organic ligands formally known as the "Schiff base from 2-pyridinecarbaldehyde and the hydrazide of 4-pyridinecarboxylic acid,"[3,4] was examined as a potential electrocatalyst for the reduction of nitrobenzene to aniline and 2,4,6-TNT to 2,4,6-triaminotoluene (TAT). This complex has been shown to electrocatalytically reduce other pollutants in wastewater. Lytvynenko et al. investigated various metal-ligand complexes, including this iron organometallic complex, as electrocatalysts for the reductive dehalogenation of organic halides.[3,4] The authors found that these metal-ligand complexes participated in these reactions as electron transfer mediators via an outer-sphere electron transfer process.[3,4] They did not discover any chemical linkage between the complexes and the organic halide substrates.

This study analyzes if the iron organometallic complex can play a role as an electrocatalyst in the reduction of nitroaromatics. Ultimately, the broader application is similar to that in Lytvynenko et al., as nitroaromatics are contaminants in wastewater streams. While Lytvynenko et al. only observed an outer-sphere mechanism, this study aims to determine if a viable inner-sphere mechanism exists for the electrocatalytic reduction of nitroaromatics by the iron organometallic complex.

Density functional theory (DFT) calculations provide insight into the energetics of elementary steps, elucidating mechanistic information about the electrocatalytic reduction of nitroaromatics by the iron organometallic complex. With knowledge of elementary step energetics, it can be discerned which reaction pathways are favored. Several theoretical studies employing DFT have been conducted to study the reduction of nitroaromatics. For instance,

Chua et al. utilized experimental measurements and theoretical calculations via DFT to identify the preferred reduction pathway of 2,4,6-TNT to 2,4,6-TAT.[5] DFT calculations confirmed that TNT reduction preferentially occurs by fully converting each nitro group to an amine before reducing the next nitro group. Additionally, Chua et al. determined that the two nitro groups ortho to the methyl group are reduced before the para nitro group.[5] In another study, He et al. used DFT to investigate the major oxidative decomposition pathways for TNT.[6] They found the dominant degradation mechanism to be oxidizing the methyl group to an aldehyde and one of the ortho nitro groups to an alcohol.

This study aims to examine the catalytic activity of the iron organometallic complex and its role in reducing toxic nitroaromatic compounds to benign aromatic amine products. First, the influence of the oxidation states of the catalyst on its activity and stability are described. After establishing the redox properties of the catalyst, complexation of nitroaromatic substrates to the catalyst is described. Using DFT, the elementary step energetics for the electrocatalytic reduction of nitrobenzene and TNT are calculated. From these calculations, inner-sphere mechanisms for both reductions are presented. The iron organometallic catalyst facilitates the steps that limit the rate of the uncatalyzed, outer-sphere reduction mechanism. Finally, ligand substitutions were made to the complex to study how this affects the activity of the catalyst.

Chapter 2

Methods

DFT calculations were carried out using the Vienna ab initio simulation package (VASP).[7-10] The projector augmented wave (PAW) method with the Perdew, Burke, and Ernzerhof (PBE) generalized gradient approximation (GGA) functional was selected.[11-14] The plane-wave basis set energy cutoff was set to 450 eV. A convergence criterion of 10^{-5} eV (EDIFF) was used for the electronic relaxation steps while the atomic force criterion for geometry optimization was 0.02 eV/Å (EDIFFG). The calculations were carried out with the spin unrestricted. The molecules were studied first with the lowest spin state (spin = 0 for even-electron species and spin = 1 for odd-electron species) and then the second lowest spin state (spin = 2 for even-electron species and spin = 3 for odd-electron species). The unit cell was cubic with a side length of 25 Å. An implicit solvation model, VASPSol, was implemented for the calculations in the solution-phase.[15,16] Water was used as the solvent, with a dielectric constant of 78.4 and a cutoff charge density of 0.00025 $e^-/Å^3$.

Although it is not intuitive to use a periodic basis set code to investigate a molecular system, VASP was utilized for a few reasons. First, VASP was found to execute much faster than the atomic basis set code Gaussian for the same GGA functional. Second, utilizing VASP rather than Gaussian enables direct comparison with other DFT analyses of nitroaromatic reduction catalyzed by heterogeneous catalysts. Thus, VASP allows for the direct comparison between this iron organometallic catalyst and extended metal (Fe) and metal oxide (FeO_x) surfaces for the catalytic reduction of nitroaromatics. Third, it was found that VASP provides reaction energetics comparable to those determined with the atomic basis set code Gaussian. To

validate this claim, DFT calculations were also implemented in Gaussian using the Gaussian 09 package.

The energetics in VASP were compared with the energetics in Gaussian to determine if the two codes provide similar results. The B3LYP functional in Gaussian was used to account for the exchange and correlation energies.[17-20] The basis set was 6-311++G(d,p). The calculations included entropic and zero-point vibrational energy (ZPVE) corrections. For the solution-phase calculations, the integral equation formalism variant of the Polarizable Continuum Model (IEFPCM) was used, with water as the solvent.[21] **Table 1** compares the energetics between the PBE functional in VASP and the B3LYP functional in Gaussian of key steps in the non-catalytic, gas-phase reduction of nitrobenzene to aniline. The differences in the raw numbers are marginal, which supports the claim that using VASP with the PBE functional is a valid choice for this system.

Table 1: A comparison between the VASP PBE and Gaussian B3LYP functionals using the gas-phase energetics of nitrobenzene reduction.[22] *Energies are relative to nitrobenzene in the gas phase at 0 V_{NHE} and pH = 0.*

Reaction	ΔG of reduction (eV) in PBE	ΔG of reduction (eV) in B3LYP
$NO_2 + e^- \rightarrow NO_2^-$	3.03	2.97
$NO_2^- + H^+ \rightarrow NOOH$	-2.63	-2.62
$NO_2 + H^+/e^- \rightarrow NOOH$	0.40	0.35

The reaction energetics were formulated so that the Gibbs free energies of each mechanistic step are dependent on the applied potential. **Equation 1** provides a framework for obtaining the reaction free energy to form any nitrobenzene reduction intermediate (*A*) relative to the nitrobenzene starting material.[22]

$$\Delta G_{red} = G_A + (2 - x)G_{H_2O} - G_{NB} - \frac{n}{2}G_{H_2} + n|e^-|U_{NHE} + m|e^-|U_{NHE} + m|e^-|\Delta U_{abs} \qquad (1)$$

In this equation, G_A, G_{H_2O}, G_{NB}, and G_{H_2} are the Gibbs free energies of the reduced intermediate, H_2O, nitrobenzene, and hydrogen gas. *n* is the number of coupled proton-electron pairs transferred, *m* is the number of uncoupled electrons added, U_{NHE} is the electrode potential on a NHE reference scale, and ΔU_{abs} is the absolute potential of the NHE.[22]

The binding energy E_{bind} resulting from the complexation of the nitroaromatic substrate to the iron organometallic catalyst was calculated according to **Equation 2**.

$$E_{bind} = E_{system} - E_{cat} - E_A \qquad (2)$$

In **Equation 2**, E_{system} is the Gibbs free energy of the nitroaromatic reduction intermediate bound to the iron organometallic complex, E_{cat} is the Gibbs free energy of the iron organometallic complex, and E_A is the Gibbs free energy of the nitroaromatic reduction intermediate.

Chapter 3

The Iron Organometallic Complex

3.1 The Structure of the Iron Organometallic Complex

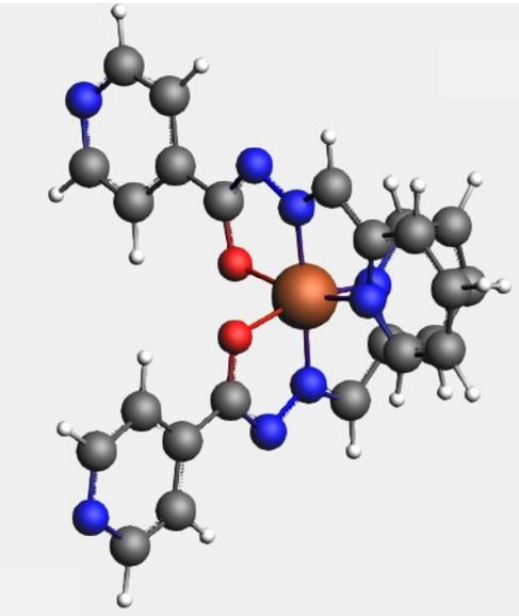

Figure 1: Chemical structure of the iron organometallic complex. *Blue = N atoms, gray = C atoms, white = H atoms, red = O atoms, and brown = Fe atoms.*

The iron organometallic complex consists of a central iron atom connected via approximately octahedral coordination to four nitrogen atoms and two oxygen atoms. It has the molecular formula $C_{24}H_{18}N_8O_2Fe$. The iron is coordinated by two chelated ligands, each contributing two N atoms and an O atom to bind to Fe. Each chelated ligand has the formula $C_{12}H_9N_4O$. The ligands serve to delocalize electron density and provide flexibility for chemical rearrangement. The iron has a formal oxidation state of +2 in this arrangement.

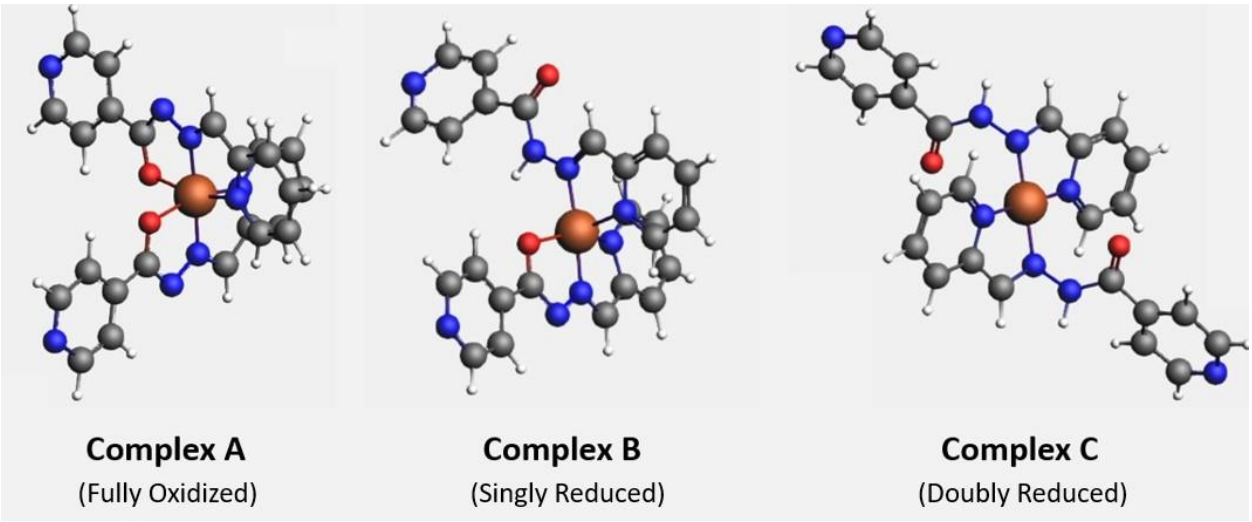

Figure 2: Optimized structures of different redox states of the iron organometallic complex

The oxidation state of the iron organometallic complex affects its catalytic activity. **Figure 2** illustrates three possible redox states of the complex, with **Complex A** being the fully oxidized state, **Complex B** being the singly reduced state, and **Complex C** being the doubly reduced state.

In general, the complex exhibits greater stability at lower spin states. The spin = 0 state, with no net unpaired electrons, is lower in energy than the spin = 2 state, with two net unpaired electrons. Additionally, when the complex is reduced, the lower spin states are still more stable than the higher spin states. **Table 2** shows the differences in energy between the lower and higher spin states for different variations of the iron organometallic complex.

Table 2: Effect of spin on the stability of the iron organometallic complex. *The energy difference refers to the energy of the higher spin state complex minus the energy of the lower spin state. This indicates how much more stable the lower spin state is. These values are without solvation.*

Complex State	Iron Oxidation State	Spin States	Energy Difference (eV)
Oxidized (A)	+2	Spin 0 to 2	0.734
Partially Reduced (B)	+1	Spin 1 to 3	1.215
Reduced (C)	0	Spin 0 to 2	0.052

3.2 Catalyst Activity and Behavior: Oxidation States and Ligand Reorientation

While **Complex A** is stable at electrochemical potentials of interest for nitroaromatic reduction, this oxidized state has six atoms coordinated to iron, preventing nitrobenzene from interacting with the iron atom via an inner-sphere mechanism; there is no open coordination site on the iron atom. Reducing **Complex A** to **Complex B**, though requiring an overpotential relative to the nitrobenzene reduction overpotential ($\Delta G = 0.82$ eV in vacuum, at 0 V_{NHE}), frees a coordination site for nitrobenzene binding by causing reorientation of the ligand and dissociation of an iron-ligand bond. The reduction occurs by adding an electron-proton pair to the beta nitrogen with respect to the iron atom. When the electron-proton pair is added, the bond between the beta nitrogen and carbon that was nominally second order becomes a single bond. To prevent this carbon from being undersaturated, the oxygen bound to the iron atom detaches, forming a carbonyl. Thus, only five atoms remain bound to the iron, and **Complex B** can bind to the nitroaromatic reactant. **Figure 3** illustrates the reduction reaction from **Complex A** to **Complex B**.

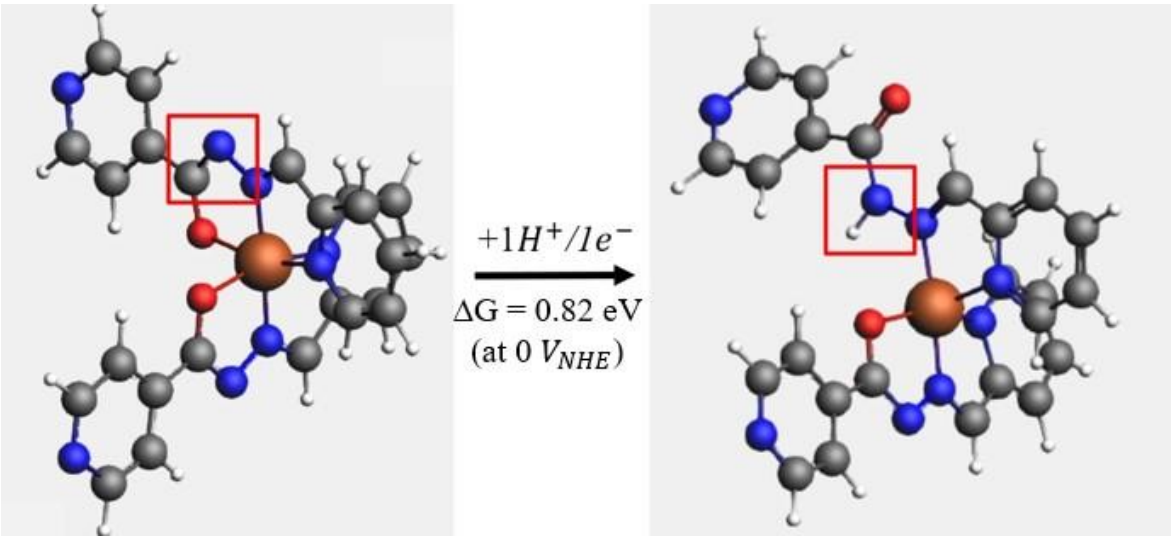

Figure 3: First reduction of the iron organometallic complex

Figure 4 and **Table 3** compare the distances of key bonds in **Complex A** and **Complex B**. The Fe-O bond in **Complex A** is relatively long at 1.972 Å, making it susceptible to dissociation when an electron-proton pair is transferred to the beta nitrogen. During the transition from **Complex A** to **Complex B**, a carbonyl is formed between the oxygen previously attached to iron and an adjacent carbon atom. This C-O bond shortens from 1.294 to 1.235 Å as it becomes nominally second order. Furthermore, the bond between the beta nitrogen and adjacent carbon lengthens from 1.342 to 1.383 Å, evolving from a nominally double to single bond.

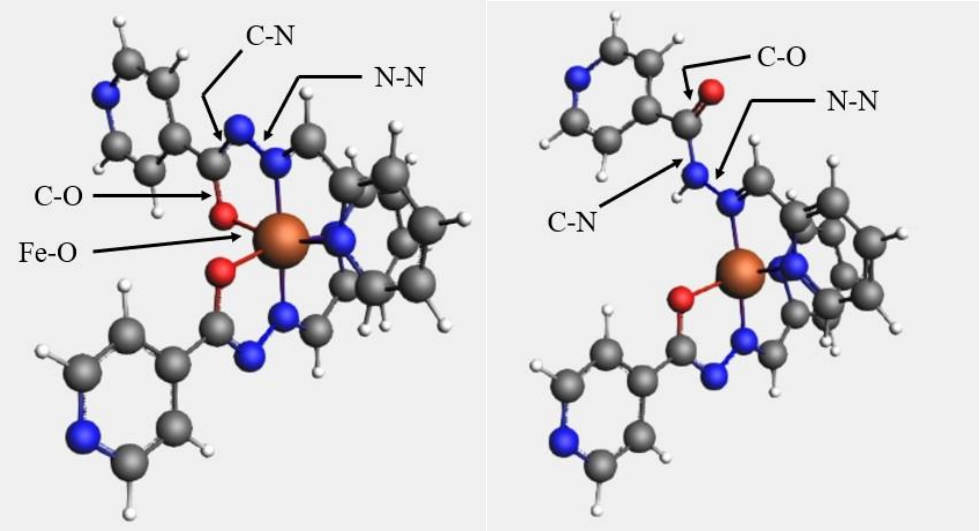

Figure 4: Key bonds in the iron organometallic complex. *Complex A is on the left while Complex B is on the right.*

Table 3: Key bond distances in the iron organometallic complex. *These key bonds are highlighted in Figure 4.*

Bond	Complex A (Å)	Complex B (Å)
Fe-O	1.972	N/A
C-O	1.294	1.235
C-N	1.342	1.383
N-N	1.357	1.375

In addition to opening up the possibility of an inner-sphere mechanism for nitroaromatic reduction, the reduction from **Complex A** to **Complex B** could facilitate an outer-sphere reaction. At -0.82 V_{NHE}, the iron organometallic complex can act as a mediator, accepting an electron/proton pair that could be shuttled to nitrobenzene or TNT.

The iron organometallic complex can undergo a further reduction, with **Complex B** being converted to **Complex C**. This mechanism follows the same pattern (see **Figure 5**), with a proton/electron pair being added to the beta nitrogen on the equivalent ligand still attached to the

iron. This induces the O from the ligand to detach from iron, leaving four atoms coordinated. The second reduction to **Complex C** requires even larger overpotentials than the first reduction to **Complex B**: the Gibbs free energy for reducing **Complex B** to **Complex C** is +1.32 eV in vacuum at 0 V_{NHE}. Furthermore, the one open coordination site in **Complex B** is sufficient for an inner-sphere mechanism; a second coordination site, like **Complex C** has, is not necessary, although it may strengthen the complexation between the iron and nitroaromatic substrate. The large reductive overpotential needed to form **Complex C** suggests it is not a viable catalyst for nitroaromatic reduction.

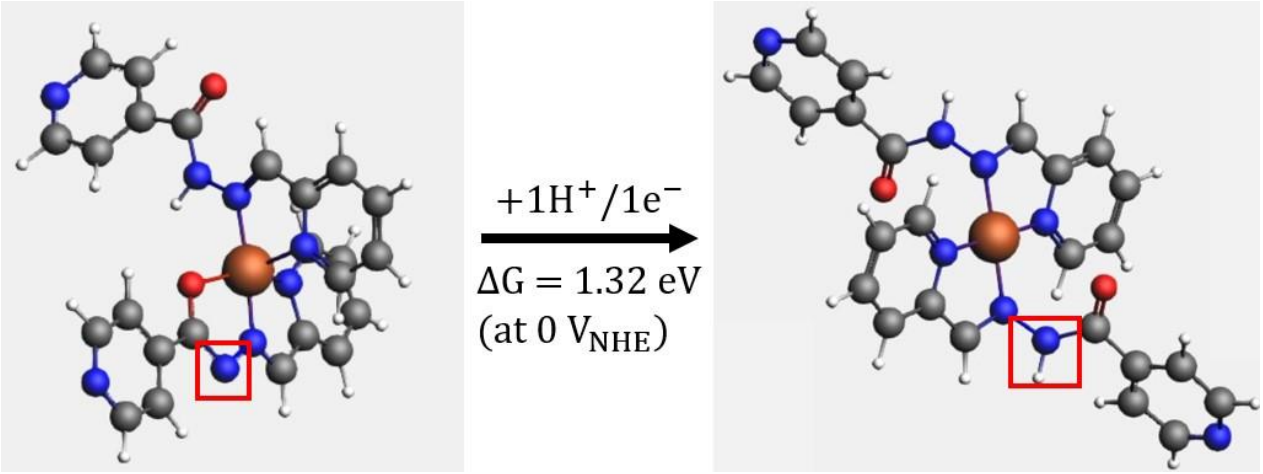

Figure 5: Second reduction of the iron organometallic complex

Lytvynenko et al. examined the energetics of adding an electron to the iron organometallic complex and similar complexes with different metal centers.[3] They used DFT calculations with the TPSS exchange-correlation potential. From their findings, the equilibrium potential associated with adding the first electron to the iron organometallic complex (**Complex A**) was -1.07 V on an NHE scale. The equilibrium potential for adding the second electron varied between -1.72 to -1.57 V on an NHE scale.[3,4] These values appear to be in agreement with the calculated equilibrium potentials of -0.82 V_{NHE} for converting **Complex A** to **Complex B** and -

1.32 V_{NHE} for converting **Complex B** to **Complex C**. However, additional work is needed before a direct comparison can be made since (1) the potentials in Lytvynenko et al. refer to only electron addition and not coupled electron-proton addition, and (2) the potentials in Lytvynenko et al. were analyzed using the COSMO continuum solvation model with DMF as the solvent.[3,4]

Chapter 4

Electrocatalytic Reduction of Nitrobenzene

4.1 Non-Catalyzed Reduction of Nitrobenzene

Nitrobenzene can undergo a reduction to aniline, in which the nitro group is converted to an amine. If run electrochemically, this reaction entails adding six electrons and protons to the nitro group. Two molecules of water are formed as byproducts of the reduction. There are two stable intermediates: nitrosobenzene (R-NO) and phenylhydroxylamine (R-NHOH), which is the major product at pH > 4.[1]

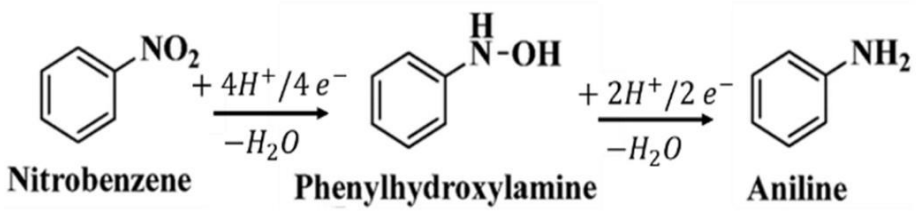

Figure 6: Reduction scheme for nitrobenzene to aniline. *Phenylhydroxylamine is the selective partial reduction product of nitrobenzene.*

Figure 7 depicts the complete non-catalytic reduction pathway for nitrobenzene to aniline in the solution-phase.[22] The full mechanism with uncoupled electron/proton transfer and each reduction intermediate is shown. The overall reaction is thermodynamically downhill, with a Gibbs free energy of -4.17 eV at 0 V_{NHE}.[22] This gives an equilibrium potential of 0.70 V_{NHE} for this six-electron reduction. If electron-proton transfer is treated as coupled for the non-catalyzed pathway, the rate-limiting step is the reduction of nitrobenzene to the R-NOOH intermediate, with a reaction energy of 0.33 eV at 0 V_{NHE}. Meanwhile, if electron-proton addition is uncoupled, the rate-limiting step is the addition of the electron to nitrobenzene, with a reaction

energy of 1.06 eV at 0 V_{NHE}. Given these observations, a catalyst for nitrobenzene reduction should optimally be designed to facilitate these rate-determining steps.

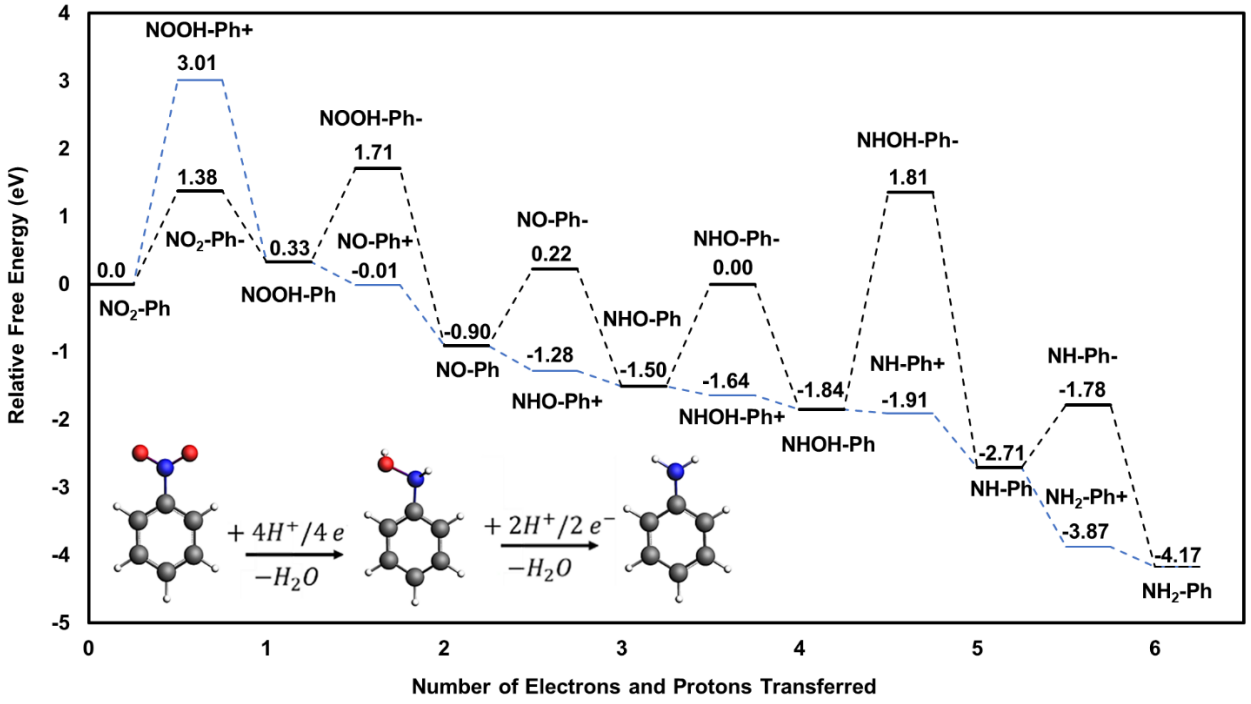

Figure 7: Non-catalytic solution-phase reduction pathway for nitrobenzene to aniline.[22]
Energies are relative to nitrobenzene in the solution-phase, at 0 V_{NHE} and pH = 0. Black dotted lines represent uncoupled electron transfer. Blue lines represent initial uncoupled proton transfer.

4.2 Complexation of Nitrobenzene with the Catalyst

After reducing **Complex A** to **Complex B**, a coordination site is opened, and complexation can occur between nitrobenzene and the iron organometallic complex. This takes place via the formation of a bond between the oxygen atom in the nitro group of nitrobenzene and the central iron atom in **Complex B** (see **Figure 8**). This complexation is associated with a binding energy of -0.73 eV in vacuum, indicating that the interaction between **Complex B** and nitrobenzene provides significant energetic stabilization. **Table 4** in the Appendix contains the

binding energies between **Complex B** and all of the reaction intermediates in the reduction of nitrobenzene.

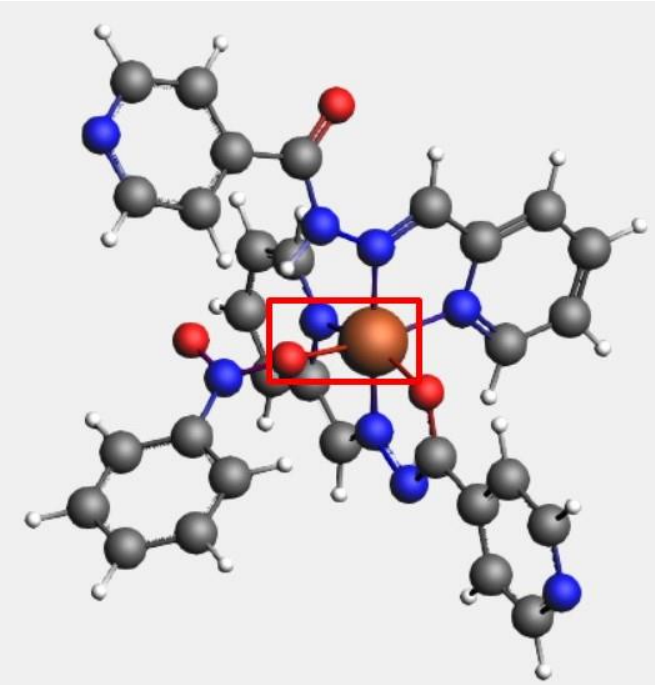

Figure 8: Nitrobenzene bound to the catalyst

There exists a trade-off between the stability of the iron organometallic complex and its activity: the more reduced the iron organometallic complex is, the more favorable nitroaromatic complexation becomes. At the same time, though, the more reduced the complex is, the less stable it becomes and the more difficult it is to obtain without resorting to large overpotentials.

While the favorable binding energy between nitrobenzene and **Complex B** suggests that an inner-sphere mechanism could occur, an outer-sphere mechanism is also possible. Comparing the reducibility of nitrobenzene versus the catalyst, the coupled electron-proton addition to nitrobenzene is only uphill by 0.33 eV. However, adding an electron and proton to **Complex A** to form **Complex B** is uphill in energy by 0.82 eV. As a result, nitrobenzene is more reducible

than the catalyst, and so the catalyst could serve as a mediator for passing electrons and protons rather than being part of an inner-sphere mechanism.

4.3 Reaction Energetics of Electrocatalytic Reduction of Nitrobenzene

While an outer-sphere mechanism is plausible, an inner-sphere mechanism for the catalytic reduction of nitrobenzene by the iron organometallic complex was still investigated to determine its feasibility. **Figure 9** shows the reduction pathway in vacuum. The nitrobenzene reduction reaction path with coupled electron-proton transfer, at relatively small overpotentials, shows an overall downward energy trend with each subsequent reduction.

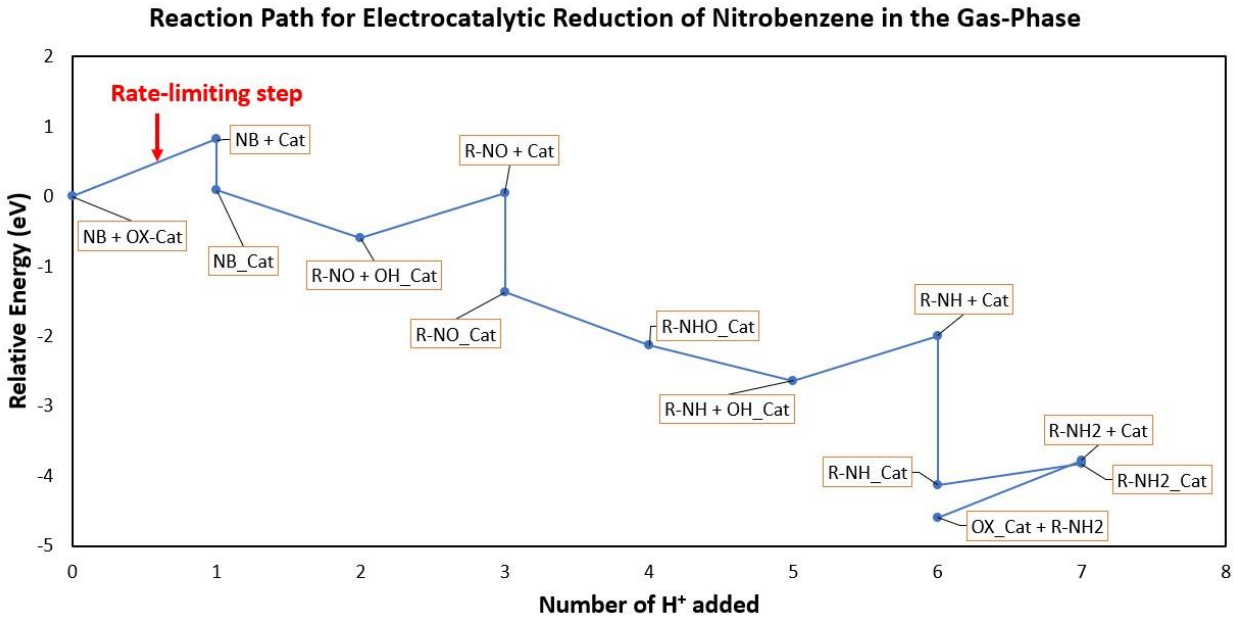

Figure 9: Electrocatalytic reduction path for nitrobenzene to aniline at 0 V_{NHE}. *NB refers to nitrobenzene, OX-Cat refers to Complex A, Cat refers to Complex B, R denotes the phenyl group in each reaction intermediate, and an underscore indicates each reaction intermediate being bound to the catalyst.*

In the catalytic reduction mechanism, the first step is to reduce the catalyst **Complex A** to **Complex B** to create an open coordination site. After this, nitrobenzene binds to the catalyst,

lowering the energy of the system. Adding an electron-proton pair creates the phenyl-NOOH intermediate. One of the nitrogen-oxygen bonds readily dissociates, creating the phenyl-NO intermediate, nitrosobenzene, and leaving OH bound to **Complex B**. Next, an electron-proton pair is added to form a water molecule and remove it from **Complex B**. The nitrosobenzene intermediate then reattaches to **Complex B** and is reduced to a phenyl-NHO intermediate. The phenyl-NHO intermediate is lower in energy than phenyl-NOH, and thus, its formation is preferred. Adding the next electron-proton pair produces phenylhydroxylamine (phenyl-NHOH), which readily splits up into the phenyl-NH intermediate plus OH on the catalyst. OH is reduced off of the catalyst by adding an electron-proton pair to form the second molecule of water. Finally, the phenyl-NH intermediate binds to **Complex B** and is then reduced to aniline (phenyl-NH_2). Aniline detaches from **Complex B** and **Complex B** is oxidized back to the original state, **Complex A**, to complete the mechanism.

From **Figure 9**, the iron organometallic catalyst facilitates the rate-limiting step in the non-catalyzed pathway, the initial reduction of nitrobenzene to the phenyl-NOOH intermediate; the transition with the catalyst from nitrobenzene to phenyl-NOOH is downhill in energy. However, there are still some uphill steps in the inner-sphere reduction with coupled proton-electron transfer. The rate-limiting step is the initial activation of the catalyst via the reduction of **Complex A** to **Complex B**. This step has a reaction energy of 0.82 eV at 0 V_{NHE}. Additionally, the mechanistic steps involving removing OH from the catalyst are difficult, with a reaction energy of 0.64 eV at 0 V_{NHE} to add an electron-proton pair and produce water. This is due to the oxophilicity of iron: iron binds very strongly to oxygen and this can result in poisoning of the catalyst by OH.

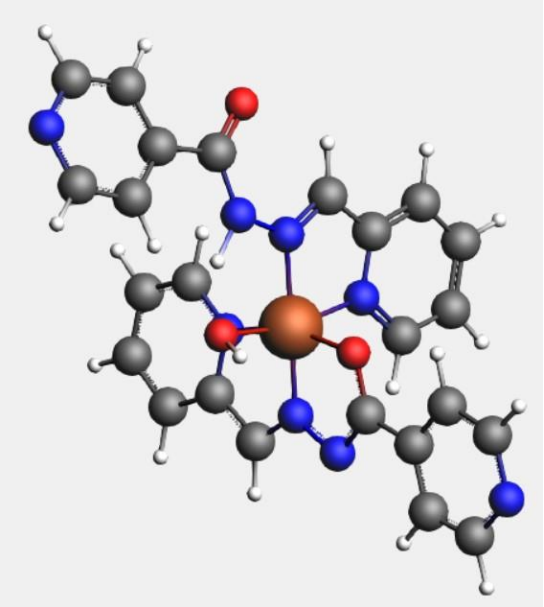

Figure 10: OH occupying the iron atom on the catalyst

4.4 Ligand Substitutions to Reduce Overpotentials in Catalytic Nitrobenzene Reduction

The rate-determining step in the electrocatalytic reduction of nitrobenzene is the reduction of the catalyst. To decrease the overpotential required to facilitate this step, electron withdrawing groups can be substituted onto the ligands of the catalyst. For instance, nitro and chloride side groups can be added to the ligands to delocalize electron density, stabilizing the singly reduced **Complex B**, and lowering the energy gap between **Complex B** and the more stable **Complex A**. Adding eight chlorine atoms across the ligands reduces the energy gap from 0.82 eV to 0.68 eV at 0 V_{NHE} (see **Figure 11**). Adding eight nitro groups across the ligands reduces the energy gap even further, from 0.82 eV to 0.47 eV at 0 V_{NHE} (see **Figure 12**). However, this may not be relevant for nitroaromatic reduction because it would be difficult to selectively reduce the nitro groups on nitrobenzene with nitro groups already on the ligands.

Thus, the nitro-substituted complex may be catalytically useful for other reactions, but not nitroaromatic reduction.

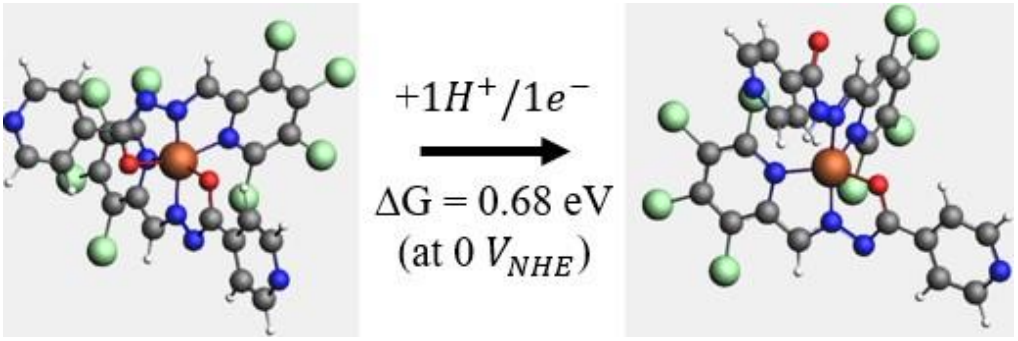

Figure 11: Reduction of the catalyst with chlorine-substituted ligands. *The atoms in green are chlorine atoms.*

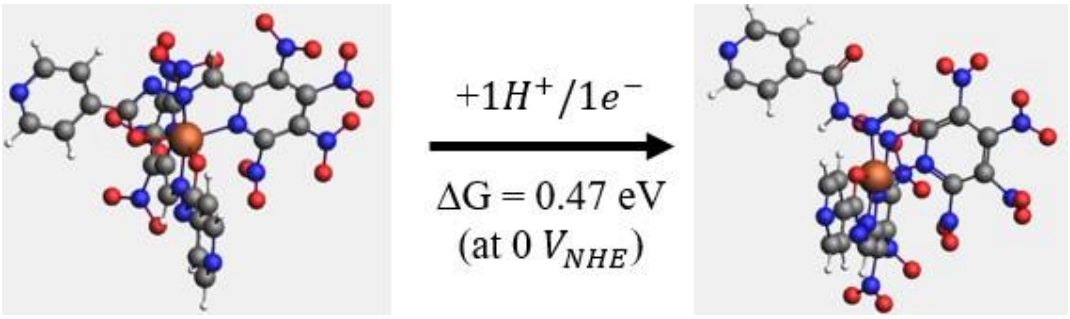

Figure 12: Reduction of the catalyst with nitro-substituted ligands

Chapter 5

Electrocatalytic Reduction of TNT

5.1 Non-Catalyzed Reduction of TNT

The electrochemical reduction of trinitrotoluene (TNT) to 2,4,6-triaminotoluene (TAT) proceeds in a similar mechanism to the reduction of nitrobenzene to aniline. 18 protons and electrons are added to TNT to convert the three nitro groups to amines. Six molecules of water are formed, along with the main product, TAT. In the non-catalytic reduction mechanism, the most energetically favorable pathway entails each nitro group being fully converted to an amine before the next one is reduced. The overall reaction is downhill in free energy by -14.32 eV, at 0 V_{NHE} in vacuum. Given that TNT conversion to TAT is an 18-electron reduction, the equilibrium potential is 0.80 V_{NHE}. **Figure 14** illustrates the non-catalytic pathway in the solution-phase for the reduction of the first nitro group in TNT, one of the nitro groups ortho to the methyl group. From **Figure 14**, the reaction energetics for uncatalyzed TNT reduction are similar to uncatalyzed nitrobenzene reduction; the relative energy of the system generally decreases, but some of the initial steps are difficult. If electron-proton transfer is treated as coupled, the rate-determining step in the reduction of the first nitro group is the reduction of TNT to the DNT-NOOH intermediate, with a reaction energy of 0.23 eV at 0 V_{NHE}.

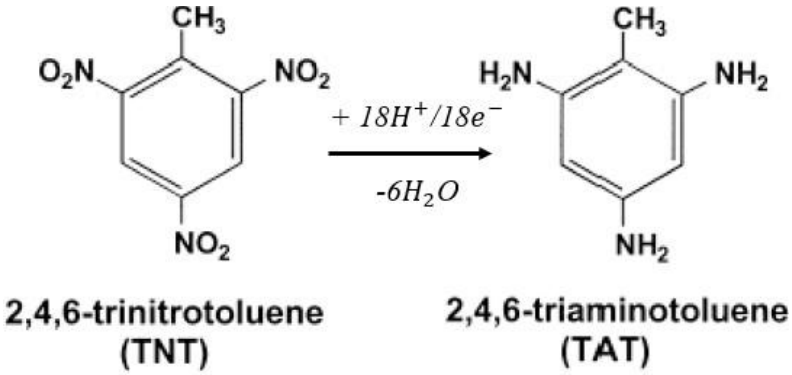

Figure 13: Reduction scheme for TNT to TAT

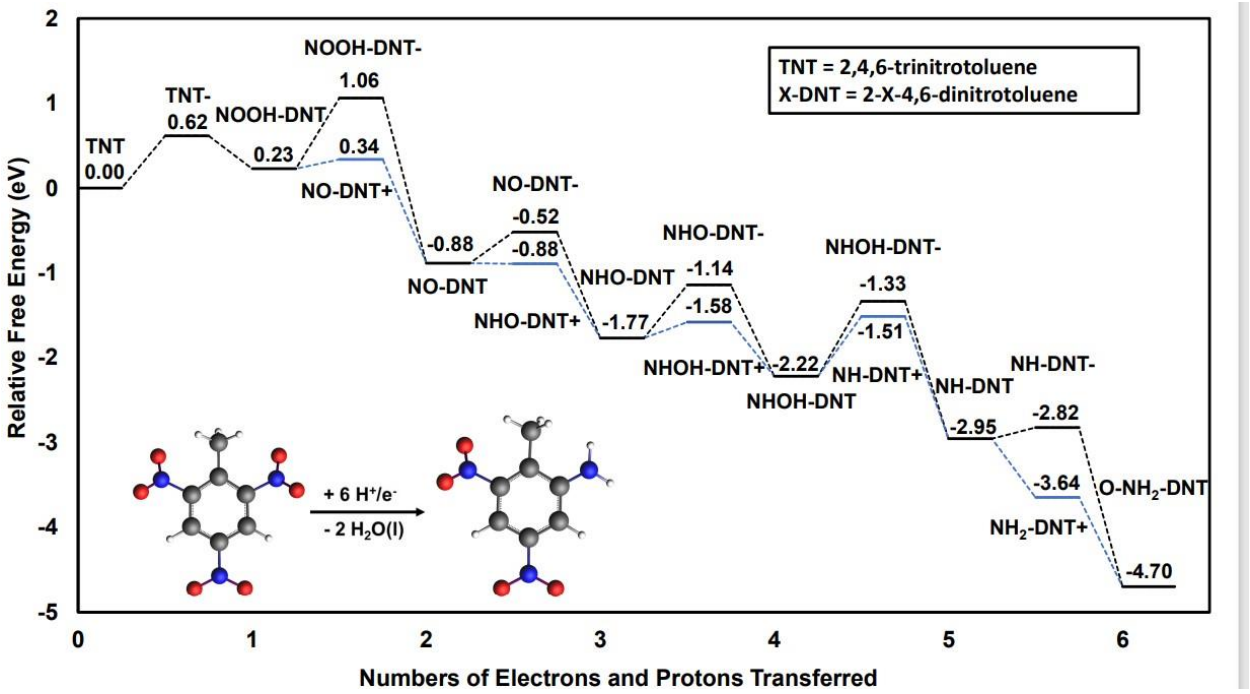

Figure 14: Non-catalytic solution-phase pathway for the reduction of the first nitro group in TNT.[22] *Energies are relative to TNT in the solution-phase, at 0 V_{NHE} and pH = 0. Black dotted lines represent uncoupled electron transfer. Blue lines represent uncoupled proton transfer. DNT refers to dinitrotoluene. The product of this six-electron reduction is o-NH_2-DNT, with nitro groups in the ortho and para positions relative to the methyl group and an amine group in the other ortho position.*

5.2 Complexation of TNT with the Catalyst

TNT complexation with the catalyst must be preceded by the reduction of **Complex A** to **Complex B** to generate an open coordination site. The optimal configuration for TNT binding to

Complex B involves bond formation between the iron atom in the catalyst and the oxygen atom on one of the nitro groups ortho to the methyl group in TNT. In vacuum, this interaction results in a binding energy of -0.76 eV. The energetic stabilization conferred by TNT binding to the catalyst is similar to that of nitrobenzene binding, which has a binding energy of -0.73 eV.

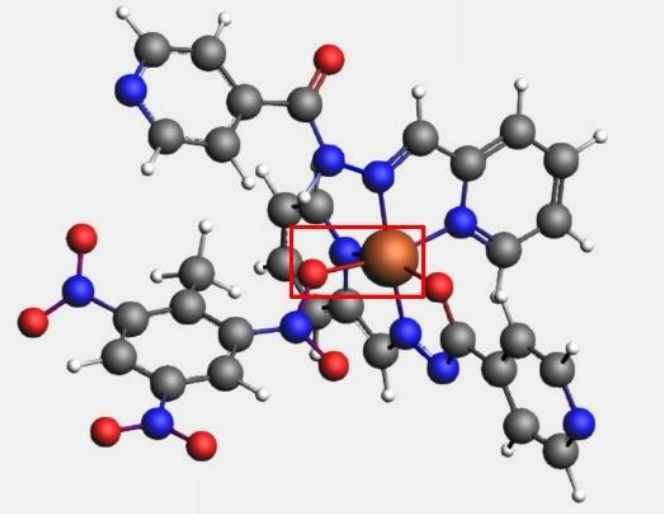

Figure 15: TNT complexed to the catalyst

5.3 Reaction Energetics of Electrocatalytic Reduction of TNT

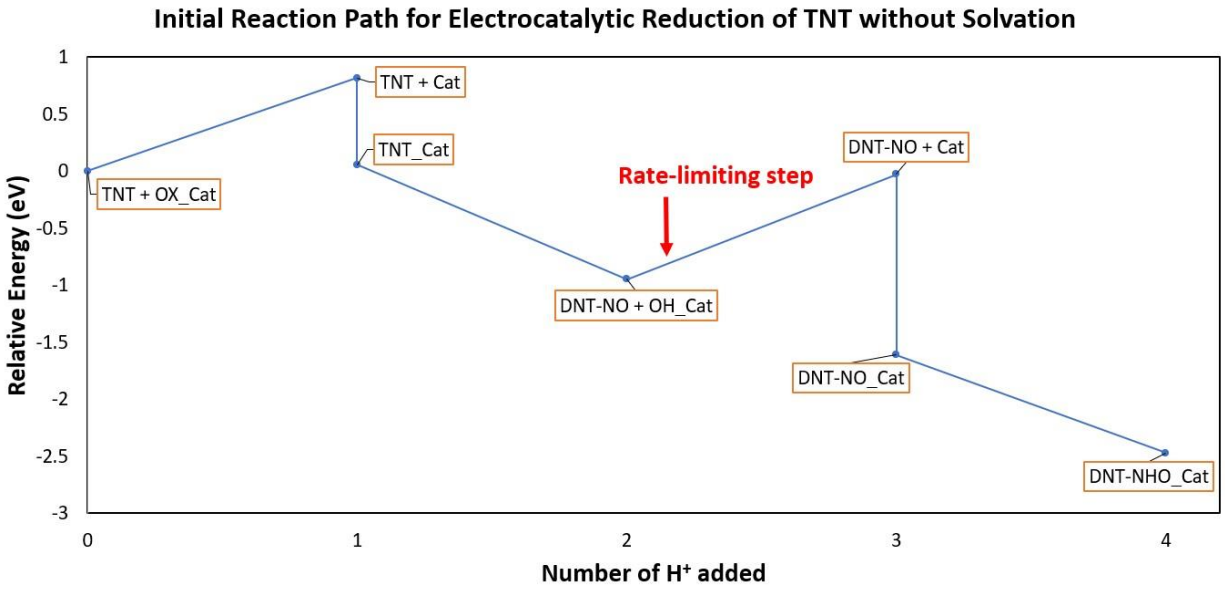

Figure 16: Initial electrocatalytic reduction path for TNT to TAT in vacuum at 0 V_{NHE}. *DNT refers to dinitrotoluene.*

The mechanism for electrocatalytic TNT reduction closely follows that of nitrobenzene reduction, with the first step being the reduction of **Complex A** to **Complex B** so that TNT can bind to the catalyst. Following this step, the reduction of TNT on the catalyst proceeds sequentially with each electron-proton pair addition. The rate-limiting step is the removal of OH off of the catalyst via the addition of an electron-proton pair to form water. This step carries a reaction energy of 0.97 eV in vacuum, compared to the 0.82 eV energy jump to activate the catalyst from **Complex A** to **Complex B**. After the first nitro group in TNT is fully converted to an amine, the mechanism repeats itself for each of the other two nitro groups. Overall, the reaction path for electrocatalytic TNT reduction demonstrates a similar trend to electrocatalytic nitrobenzene reduction, with the initial catalyst activation and OH removal steps appearing difficult, but the relative energy of the system mostly decreasing. Additionally, the iron

organometallic complex facilitates the rate-limiting step in the uncatalyzed mechanism, the electron-proton addition to TNT to form DNT-NOOH.

Chapter 6

Conclusions and Future Work

This work has been the first to elucidate the unique catalytic activity of this iron organometallic complex. In its oxidized state, **Complex A**, the iron organometallic complex does not have any open coordination sites. However, addition of an electron-proton pair to the complex induces ligand rearrangement and dissociation of an oxygen-iron bond, freeing a coordination site for substrate binding. The resultant complex, **Complex B**, is a viable electrocatalyst for the inner-sphere reduction of nitroaromatics. **Complex B** helps promote the electroreduction of nitrobenzene to aniline and TNT to TAT. More specifically, it facilitates the rate-limiting steps in the non-catalyzed pathways, the initial reduction of the nitroaromatic substrate. The rate-limiting step for catalytic nitrobenzene reduction is the initial reduction of the catalyst while the rate-limiting step for catalytic TNT reduction is removal of OH from the catalyst. Outside of the rate-limiting steps, the catalytic reduction profiles for TNT and nitrobenzene follow an overall downward energy trajectory.

Future analysis to expand on this work includes obtaining the catalytic reduction mechanism of TNT and nitrobenzene with uncoupled electron-proton transfer – adding the electron and proton separately. It would be interesting to assess whether adding an electron to **Complex A** results in the opening of a coordination site on iron or if the electron-proton pair is necessary to cause ligand rearrangement. Additionally, data for the uncoupled electron addition to the iron organometallic complex would provide a better benchmark for comparison with the existing literature; Lytvynenko et al. stated the equilibrium potentials for adding just an electron

to the iron organometallic complex.[3,4] Along with determining the uncoupled inner-sphere catalytic mechanism, the possibility of an outer-sphere mechanism for catalytic nitroaromatic reduction needs to be explored. Instead of merely opening a coordination site for substrate binding, the reduction of **Complex A** to **Complex B** can be thought of as a mechanism for storing an electron and proton on the catalyst. This electron-proton pair could plausibly be transferred to the nitroaromatic substrate without the substrate ever binding to the catalyst. Additional further work includes developing a microkinetic model for catalytic nitroaromatic reduction and investigating if other nitroaromatic substrates can be catalyzed by the iron organometallic complex. More detailed analysis will also focus on the effects of solvation on the catalytic reduction mechanisms and the complexation between the catalyst and nitroaromatic substrate.

BIBLIOGRAPHY

1. Rodgers, J. D., and Bunce, N.J. (2001). Electrochemical Treatment of 2,4,6 Trinitrotoluene and Related Compounds. Environ. Sci. Technol. *35*, 406–410.
2. Wang, J., Yuan, Z., Nie, R., Hou, Z., Zheng, X. (2010). Hydrogenation of Nitrobenzene to Aniline over Silica Gel Supported Nickel Catalysts. Ind. Eng. Chem. Res., *49*, 4664-4669.
3. Lytvynenko, A.S., Kolotilov, S.V., Kiskin, M.A., Eremenko, I.L., Novotortsev, V.M. (2015). Modeling of catalytically active metal complex species and intermediates in reactions of organic halides electroreduction. Phys. Chem. Chem. Phys., *17*, 5594-5605.
4. Lytvynenko, A.S., Kolotilov, S.V., Kiskin, M.A., Cador, O., Golhen, S., Aleksandrov, G.G., Mishura, A.M., Titov, V.E., Ouahab, L., Eremenko, I.L., Novotortsev, V.M. (2014). Redox-Active Porous Coordination Polymers Prepared by Trinuclear Heterometallic Pivalate Linking with the Redox-Active Nickel(II) Complex: Synthesis, Structure, Magnetic and Redox Properties, and Electrocatalytic Activity in Organic Compound Dehalogenation in Heterogeneous Medium. Inorg. Chem., *10*, 4970-4979.
5. Chua, C.K., Pumera, M., Rulisek, L. (2012). Reduction Pathways of 2,4,6 Trinitrotoluene: An Electrochemical and Theoretical Study. J. Phys. Chem C, *116*, 4243-4251.
6. He, X., Zeng, Q., Zhou, Y., Zeng, Q., Wei, X., Zhang, C. (2016). A DFT Study Toward the Reaction Mechanisms of TNT With Hydroxyl Radicals for Advanced Oxidation Processes. J. Phys. Chem. A, *120*, 3747-3753.

7. Kresse, G., and Hafner, J. (1993). Ab initio molecular dynamics for liquid metals. Phys. Rev. B, *47*, 558.
8. Kresse, G., and Hafner, J. (1994). Ab initio molecular-dynamics simulation of the liquid-metal-amorphous-semiconductor transition in germanium. Phys. Rev. B, *49*, 14251.
9. Kresse, G., and Furthmüller, J. (1996). Efficiency of ab-initio total energy calculations for metals and semiconductors using a plane-wave basis set. Comput. Mat. Sci., *6*, 15.
10. Kresse, G., and Furthmüller, J. (1996). Efficient iterative schemes for ab initio total energy calculations using a plane-wave basis set. Phys. Rev. B, *54*, 11169.
11. Blochl, P.E. (1994). Projector augmented-wave method. Phys. Rev. B, *50*, 17953.
12. Kresse, G., and Joubert, D. (1999). From ultrasoft pseudopotentials to the projector augmented-wave method. Phys. Rev. B, *59*, 1758.
13. Perdew, J.P., Burke, K., and Ernzerhof, M. (1996). Generalized gradient approximation made simple. Phys. Rev. Lett., *77*, 3865.
14. Perdew, J.P., Burke, K., and Ernzerhof, M. (1997). Erratum: Generalized gradient approximation made simple. Phys. Rev. Lett., *78*, 1396
15. Mathew, K., Kolluru, V.S.C., Mula, S., Steinmann, S.N., and Hennig, R.G. (2019). Implicit self-consistent electrolyte model in plane-wave density-functional theory. arXiv:1601.03346 [cond-mat].
16. Mathew, K., Sundararaman, R., Letchworth-Weaver, K., Arias, T.A., and Hennig, R.G. (2014). Implicit solvation model for density-functional study of nanocrystal surfaces and reaction pathways. The Journal of Chemical Physics *140*, 084106.

17. Lee, C., Yang, W., and Parr, R.G. (1988). Development of the Colle-Salvetti correlation-energy formula into a functional of the electron density. Phys. Rev. B *37*, 785–789.

18. Becke, A.D. (1993). Density-functional thermochemistry. III. The role of exact exchange. J. Chem. Phys. *98*, 5648–5652.

19. Hehre, W.J., Ditchfield, R., and Pople, J.A. (1972). Self—Consistent Molecular Orbital Methods. XII. Further Extensions of Gaussian—Type Basis Sets for Use in Molecular Orbital Studies of Organic Molecules. J. Chem. Phys. *56*, 2257–2261.

20. Hariharan, P.C., and Pople, J.A. (1973). The influence of polarization functions on Molecular orbital hydrogenation energies. Theor. Chim. Acta *28*, 213–222.

21. Tomasi, J., Mennucci, B., and Cammi, R. (2005). Quantum Mechanical Continuum Solvation Models. Chem. Rev. *105*, 2999–3094.

22. Wong, A.J., Miller, J.L., Janik, M.J. (2022). Elementary mechanism for the electrocatalytic reduction of nitrobenzene on late transition metal surfaces from density functional theory. Chem Catalysis (accepted paper, waiting to be published).

Appendix A

Supplemental Figures and Tables

Table 4: Summary of binding energies for each reaction species in their lowest spin states

Reaction State	E_{bind} in vacuum (eV)	E_{bind} with VASPSol (eV)
R-NO_2_Cat	-0.73	-0.65
R-NO + OH_Cat	-1.88	-1.69
R-NO_Cat	-1.41	-1.35
R-NHO_Cat	-1.39	-1.22
R-NH + OH_Cat	-1.24	-1.18
R-NH_Cat	-2.14	-1.98
R-NH_2_Cat	-0.04	-0.12

Table 5: Summary of binding energies for each reaction species in their second-to-lowest spin states

Reaction State	E_{bind} in vacuum (eV)	E_{bind} with VASPSol (eV)
R-NO_2_Cat	-1.35	-0.53
R-NO + OH_Cat	-2.52	-1.27
R-NO_Cat	-1.74	-0.92
R-NHO_Cat	-2.01	-1.10
R-NH + OH_Cat	-1.87	-0.76
R-NH_Cat	-2.63	-1.64
R-NH_2 + Cat*	0	0

*The Fe-N bond readily dissociates upon addition of an electron and proton to R-NH_Cat in the second-to-lowest spin state. This results in aniline ($R\text{-}NH_2$) being unbound to the regenerated catalyst **Complex B**.

Academic Vita of Joshua Miller

jvm6463@psu.edu

EDUCATION

Bachelor of Science in Chemical Engineering, Minor in Mathematics

Schreyer Honors College

The Pennsylvania State University, University Park, PA

Anticipated Graduation: May 2022

Study Abroad

IES Abroad: Barcelona, Spain May - July 2019

- Enhanced my Spanish language skills and learned about Barcelona's culture while taking Spanish and history classes

TECHNICAL EXPERIENCE

Undergraduate Research Assistant

Janik Computational Catalysis Group (PSU) Aug. 2019 - present

2020 Penn State University Computational Catalysis Summer Research Program

- Apply density functional theory (DFT) and microkinetic modeling to analyze catalytic processes
- Investigate the mechanism, energetics, and kinetics of the electrocatalytic reduction of nitrobenzene by an iron organometallic catalyst
- Collaborated as a co-author with Michael Janik and Andrew Wong on a publication accepted to *Chem Catalysis* titled "Elementary mechanism for the electrocatalytic reduction of nitrobenzene on late transition metal surfaces from density functional theory"
- Presented a poster titled "Electrocatalytic Reduction of Nitrobenzene by Iron-Salen Ligand Complexes" at the 2021 AIChE Annual Meeting (Catalysis and Reaction Engineering Division) in Boston, MA
    - Co-authors: Michael Janik, Brandon Perdue, and Andrew Wong
- Delivered a presentation of my research at the 2020 Gulf Coast Undergraduate Research Symposium hosted by Rice University

Rondinelli Materials Group (Northwestern) June 2021 – present

2021 Northwestern University MRSEC REU Program

- Analyze if perovskite structures of calcium titanium sulfide and calcium titanium selenide are viable for solar absorption applications
- Utilize phonon band diagrams to assess the dynamic stability of perovskite structures and electronic band diagrams to examine their optical and electronic properties
- Presented my research findings at the summer REU symposium
- Broadened my knowledge of materials science, solid-state physics, and quantum mechanics

WORK EXPERIENCE

Instructional Aide (IA) 2020 – present

Chemical Engineering Laboratory, Chemical Reaction Engineering, Fluid Mechanics, and Material Balances (2 times)

- Assist students with the course material, holding office hours and leading exam review sessions
- Develop novel ways of explaining ideas to cater to students' needs
- Advance knowledge of chemical engineering while enriching my own understanding of key concepts and ideas
- Collaborate with the professor to develop problems and solutions

Library Page

Schlow Centre Region Library, State College, PA Feb. 2019 – May 2020

- Supervised the front desk and trained new library pages
- Organized, categorized, and shelved books

SOFTWARE

Amsterdam Density Functional (ADF), Excel, Gaussian, Materials Studio, Mathematica, MATLAB, Matplotlib, Python, SolidWorks, Unix, VASP, VESTA

LEADERSHIP

Group Leader, Chem-E-Car (PSU) 2020 - present

- Investigate the iodine clock reaction as the stopping mechanism for a small-scale, autonomous car powered by a chemical energy source
- Manage and mentor a group of students, teaching them how to carry out different experiments

Secretary, ΩXE Chemical Engineering Honor Society (PSU) 2021 - present

- Publicize important announcements and organize events
- Reestablished the organization after a long period of inactivity

Leader, National Stuttering Association (PSU Chapter) 2020 – present

- Lead discussions with other people who stutter, creating a safe environment for people to share their experiences with stuttering
- Host speakers to discuss recent advances in stuttering research

Webmaster, American Institute of Chemical Engineers (PSU) 2020 – 2021

- Maintained and updated the organization's website
- Disseminated chemical engineering-related announcements

Member, Engineers Without Borders (PSU) 2019 – 2021

- Designed a piping system to supply water to a community in Uganda

Member, Tau Beta Pi: Engineering Honor Society (PSU) 2020 – present

AWARDS

Chemical Engineering Department Undergraduate Scholarship 2020, 2021

Larry Duda Undergraduate Student Research Award 2021